

Qualitative and quantitative detection of the QCD phase-transition boundary

Zhi-Min Wu^{1,2} and Gao-Chan Yong^{1,2*}

¹*School of Nuclear Science and Technology, University of Chinese Academy of Sciences, Beijing 100049, China*

²*Institute of Modern Physics, Chinese Academy of Sciences, Lanzhou 730000, China*

In this compelling study, we delve into the intricate relationship between the Equation of State (EoS) that encompasses a “QGP-like” phase transition and the directed flow (v_1) of protons and Λ particles, specifically at beam energies under 10 GeV. Utilizing the sophisticated Multi-Phase Transport (AMPT-HC) model, our analysis not only resonates with the STAR experimental data but also reveals striking dips in the directed flow strength for both types of particles as the collision energy is ramped up. These pronounced features, which are more noticeable across various phase-transition regions within the EoS, offer invaluable insights into the presence and detailed nature of the QCD phase transition. Our findings underline the critical role of directed flow measurements in beam energy scans as effective instruments for probing and understanding the phase structure of nuclear matter in heavy-ion collisions, highlighting their potential to unlock new frontiers in high-energy nuclear physics.

Determining the phase-transition boundary and critical point within nuclear matter is vital for unraveling the development and formation of the universe [1]. High-energy heavy-ion collisions present a unique method to produce a small amount of quark-gluon plasma (QGP), thus aiding the exploration of the early stages of the universe [2–4]. Such experiments allow researchers to probe the Quantum Chromodynamics (QCD) phase diagram [5]. It is proposed that the interaction between the freeze-out trajectory and the anticipated first-order phase transition line in the QCD phase diagram may result in a softer equation of state (EoS) [6, 7]. The Beam Energy Scan (BES) program at the Relativistic Heavy Ion Collider (RHIC) at Brookhaven National Laboratory has conducted various measurements investigating the potential signs of QGP, evidence of a first-order phase transition, and the location of the critical point within QCD matter by assessing the reaction system, energy, and centrality dependence of certain observables [8, 9]. Importantly, collisions that achieve high baryonic density within the 2 to 20 GeV energy domain are deemed crucial for pinpointing the phase transition boundary [10]. Analyses from both BES-I and BES-II indicate that partonic degrees of freedom might continue to prevail even at energy levels as low as 7.7 GeV [11].

To combat the reduction in statistical relevance with lowering energy and to cover the substantial data void in the 3.0 to 7.7 GeV range regarding the non-monotonic energy dependence of high-order moments of net-proton fluctuations, the Fixed-target (FXT) project has engaged in a set of high-statistics experiments and data collection initiatives. This effort provides extremely valuable information for the study of high-density nuclear matter properties. Upcoming experiments such as those at CBM and HADES at FAIR [12, 13], BM@N and MP [14], CEE at HIAF [15], and the proposed J-PARC-HI in Japan [16] are poised to deliver significant insights into the QCD

phase diagram.

The equation of state (EoS) is a crucial physical metric that encapsulates the properties of nuclear matter, occupying a central role in both nuclear physics and nuclear astrophysics [17, 18]. Yet, formulating a precise EoS at finite chemical potentials from foundational principles remains a formidable task. Due to the significant influence of the EoS on the dynamics of heavy-ion collisions, constraints can be applied to the EoS by integrating experimental outcomes with theoretical transport models [19, 20]. Considering the importance of hadronic interactions in these collisions [21], a versatile hadronic EoS can be designed to closely represent the characteristics expected from the QCD phase transition in various models [22]. By analyzing the simulation results with a hadronic EoS that models a “QGP-like” phase transition against actual experimental observations, researchers can deduce the authentic EoS.

The anisotropic collective flow observed in high-energy heavy-ion collisions is widely employed to probe the properties of dense QCD matter at various beam energies [23]. By conducting simulations with transport models using a hadronic EoS that flexibly encapsulates the QCD phase transition characteristics, it is expected that the EoS can be pinpointed by comparing against a spectrum of experimental results from the recent RHIC-STAR FXT program. In this research, we utilize the purely hadronic transport model, AMPT-HC [24], by integrating the EoS with diverse baryonic phase-transition scenarios to explore the potential QCD phase transition at FXT energies through the analysis of proton and Λ directed flows.

The Multi-Phase Transport model (AMPT) is extensively utilized for simulating heavy-ion collisions within the energy spectra of RHIC and LHC [25], owing to its comprehensive portrayal of both hadronic and partonic states during collisions. As a Monte Carlo-based model, AMPT includes four key elements: initializing fluctuating initial states, interactions among partons, the conversion from partons to hadrons during hadronization, and interactions between hadrons [26]. The goal of this study is to investigate the EoS featuring a “QGP-like”

*Corresponding author: yonggaochan@impcas.ac.cn

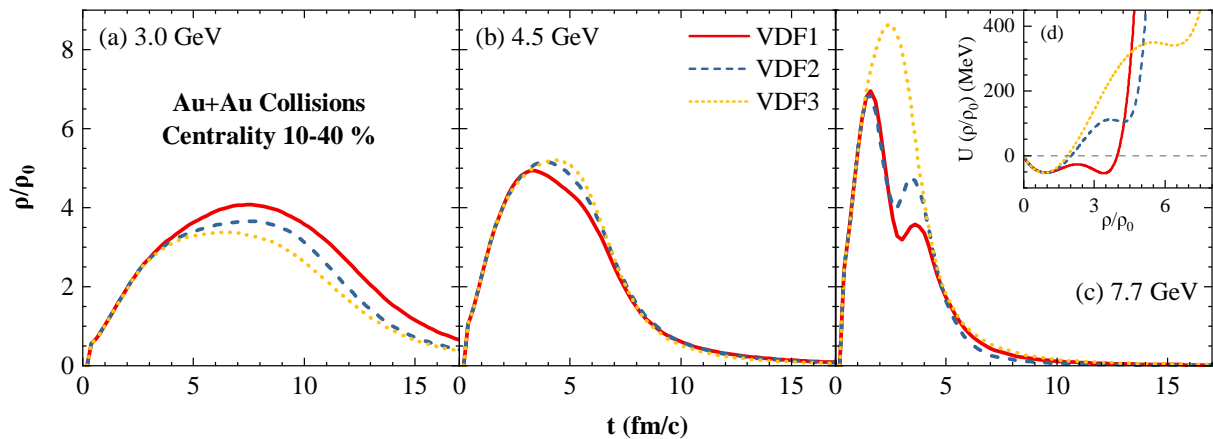


FIG. 1: Evolution of the maximum compressed baryonic density in semicentral Au+Au collisions using various EoSs at $\sqrt{s_{NN}} = 3$ GeV (a), 4.5 GeV (b), and 7.7 GeV (c). Inset panel (d) displays the single-particle potentials for different VDF EoSs as a function of baryonic density.

phase transition within the FXT energy range, employing the purely hadronic mode of AMPT, known as AMPT-HC. Operating predominantly with hadronic mechanics, the AMPT-HC model [24] uses the Woods-Saxon nuclear density profile and a local Thomas-Fermi approximation to set up the initial phase-space distributions of nucleons in both the projectile and target nuclei. It manages nucleon collisions and transportations through hadronic potentials and the test particle method, involving nucleons, baryon resonances, strange particles, and their corresponding antiparticles. Details regarding the operative mechanisms and the hadron cascade process in AMPT-HC are discussed in several references including [26–30].

The relativistic vector density function (VDF) model based on Landau Fermi-Liquid theory utilizes phenomenological parameters to capture the deviation of a system from equilibrium. These parameters include excitation energy, particle interactions, and bulk system properties [22, 31, 32]. Although the phase transition within the Landau Fermi-Liquid model doesn’t affect the degrees of freedom, maintaining a hadronic scope, the VDF model can produce a phase diagram replicative of the actual QCD phase transition and describe the EoS for high-density nuclear matter accurately. The single-particle potential in a VDF framework is determined by setting constraints like the extremum of binding energy at saturation density, the critical points of nuclear liquid-gas $(T_c^{(N)}, n_c^{(N)})$ and QCD phase transitions $(T_c^{(Q)}, n_c^{(Q)})$, and the limits of the zero-temperature QCD phase transition spinodal region (η_L, η_R) . The potential is given by the following expression [33]:

$$U = \sum_{i=1}^N \tilde{C}_i \left(\frac{\rho}{\rho_0}\right)^{b_i-1}. \quad (1)$$

Here, \tilde{C}_i and b_i represent the coefficients of VDF, whereas ρ and ρ_0 refer to the baryon number density and its saturation point, respectively. The coefficients for differ-

ent EoSs (VDF1, VDF2, and VDF3) can be found in Ref. [33]. These different EoSs or single-particle potentials are depicted in Figure 1 (d), where extremum points in the single-nucleon potentials indicate phase transitions at particular densities — ranging for VDF1, VDF2, and VDF3 at baryon density intervals of $2.5 \sim 3.5$, $3.5 \sim 4.5$, and $5.0 \sim 6.5\rho/\rho_0$, respectively. Utilizing these VDF EoSs along with simulations from transport models and experimental data from heavy-ion collisions enables the exploration of the phase-transition boundary of QCD matter and the mapping of its phase diagram.

One of the principal physical quantities relevant to the QCD phase diagram is the peak baryonic density achieved in the FXT experiments. Figure 1 illustrates the evolution of the maximum compressed baryonic density under various phase-transition EoSs at FXT energies. The graph shows that the maximum compressed baryonic density tends to increase with rising beam energy. The soft/stiff EoSs — VDF1/VDF3 at lower energies and VDF3/VDF1 at higher energies — yield higher and lower baryonic densities, respectively. Different compression levels of nuclear matter can influence the collective flow properties of protons or Λ particles.

The directed flow v_1 , defined as the first harmonic coefficient in the Fourier expansion of the final state particle momentum distribution in heavy-ion collisions [23], is expressed by

$$v_1 = \langle \cos(\phi) \rangle = \left\langle \frac{p_x}{p_T} \right\rangle, \quad (2)$$

where p_T represents the transverse momentum, and ϕ is the azimuthal angle relative to the reaction plane. Through the analysis of v_1 for various particles, insights into the properties of dense matter can be obtained [34–39], making it a focus of both experimental and theoretical efforts.

To examine the properties of dense matter with potential “QGP-like” phase transitions, we computed the

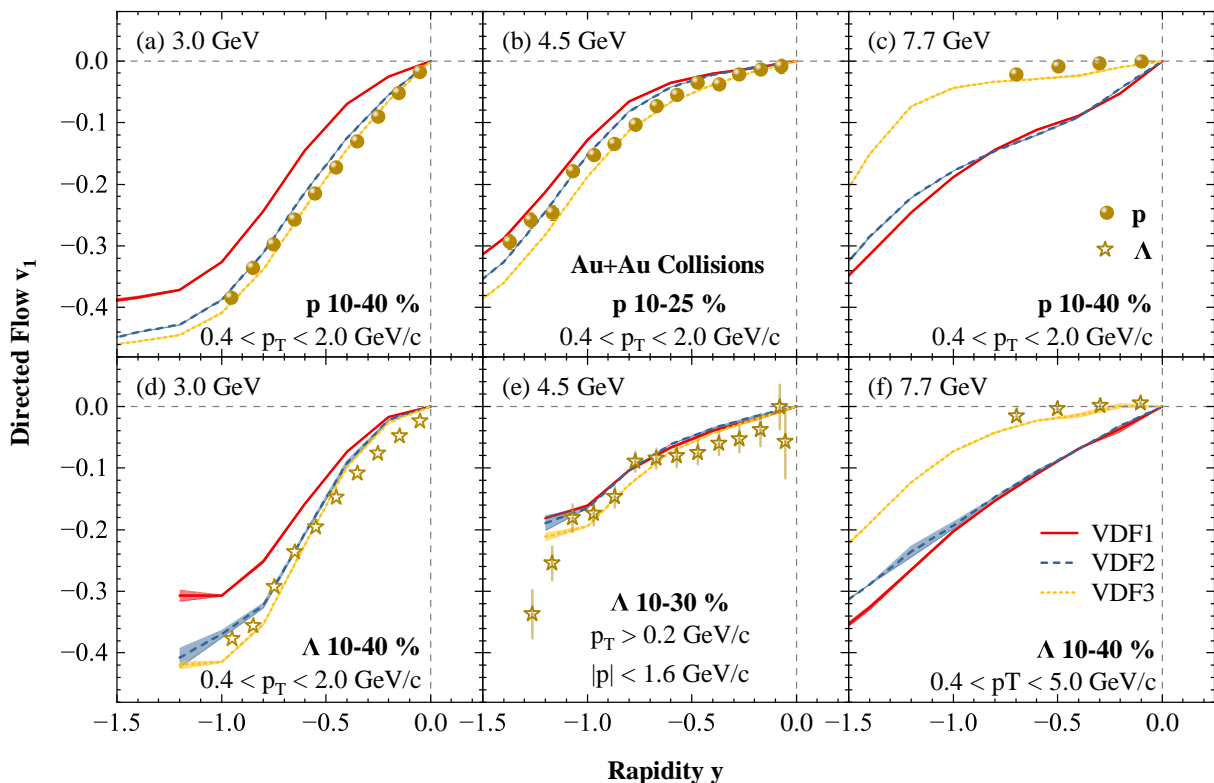


FIG. 2: Rapidity (y) dependence of directed flow v_1 for protons (upper panels) and Λ hyperons (lower panels) in the semicentral Au+Au collisions at $\sqrt{s_{NN}} = 3, 4.5,$ and 7.7 GeV, calculated using AMPT-HC with various VDF EoSs. Experimental data for protons and Λ hyperons, provided by the RHIC-STAR collaboration (Refs. [40–43]), are represented by gold spheres and stars, respectively.

rapidity-dependent v_1 for proton and Λ across different energies using various VDF EoSs, as shown in Figure 2. By correlating the maximum compressed baryonic densities at these energies, illustrated in Figure 1, one observes a clear relationship between the strengths of the directed flows v_1 of proton or Λ and the peak compressed densities across different phase-transition EoSs. Supported by experimental data, collisions from 3.0 to 7.7 GeV display distinct behaviors in Figure 2. Notably, at 3.0 GeV, no phase transition is apparent; the situation remains ambiguous at 4.5 GeV; however, by 7.7 GeV, the necessity for a phase transition becomes evident.

However, as is widely known, any model study results come with theoretical uncertainties, and the calculated directed flows of protons and Λ hyperons are no exception. Is there a method that can firstly qualitatively detect the presence of a first-order hadron-quark phase transition, and then pinpoint the location of the transition point specifically? This is an extremely important and worthwhile issue to investigate.

In order to minimize the dependence of research findings on the model or specific observables, we present the variation of the directed flow strength of protons and Λ hyperons with beam energy under different phase-transition EoSs. From Figure 3, one can see that with the three phase-transition EoSs, all the directed flow

strengths have minimum extremum points as the collision energy increases [38]. Specifically, the energy of the minimum extremum point of proton or Λ directed flow strength is ~ 4.5 GeV for the VDF1 EoS ($2.5 \sim 3.5\rho/\rho_0$ phase-transition); it is ~ 5.2 GeV for the VDF2 EoS ($3.5 \sim 4.5\rho/\rho_0$ phase-transition); and ~ 7.5 GeV for the VDF3 EoS ($5.0 \sim 6.5\rho/\rho_0$ phase-transition). By comparing Figures 1 and 3, it is easy to note that for different EoSs, such as VDF3, the collision energy $\sqrt{s_{NN}}$ corresponding to the minimum directed flow strength leads to a maximum baryon compression density that is significantly greater than the phase-transition baryonic density of VDF3. This is because the directed flow strength depends not only on the strength of the single-particle potential at maximum compression but also on the subsequent expansion (lower baryonic density) process. Therefore, the actual collision energy corresponding to minimum extremum point of the directed flow strength is always relatively higher than the expected value. It is noted that for protons and Λ hyperons, although the strengths of the flow differ numerically, the beam energies corresponding to their minimum extremum points are consistent for the same phase-transition EoS. This further demonstrates the superiority of detecting phase transitions through the analysis of minimum extremum points. From Figure 3, it is seen that, once the variation

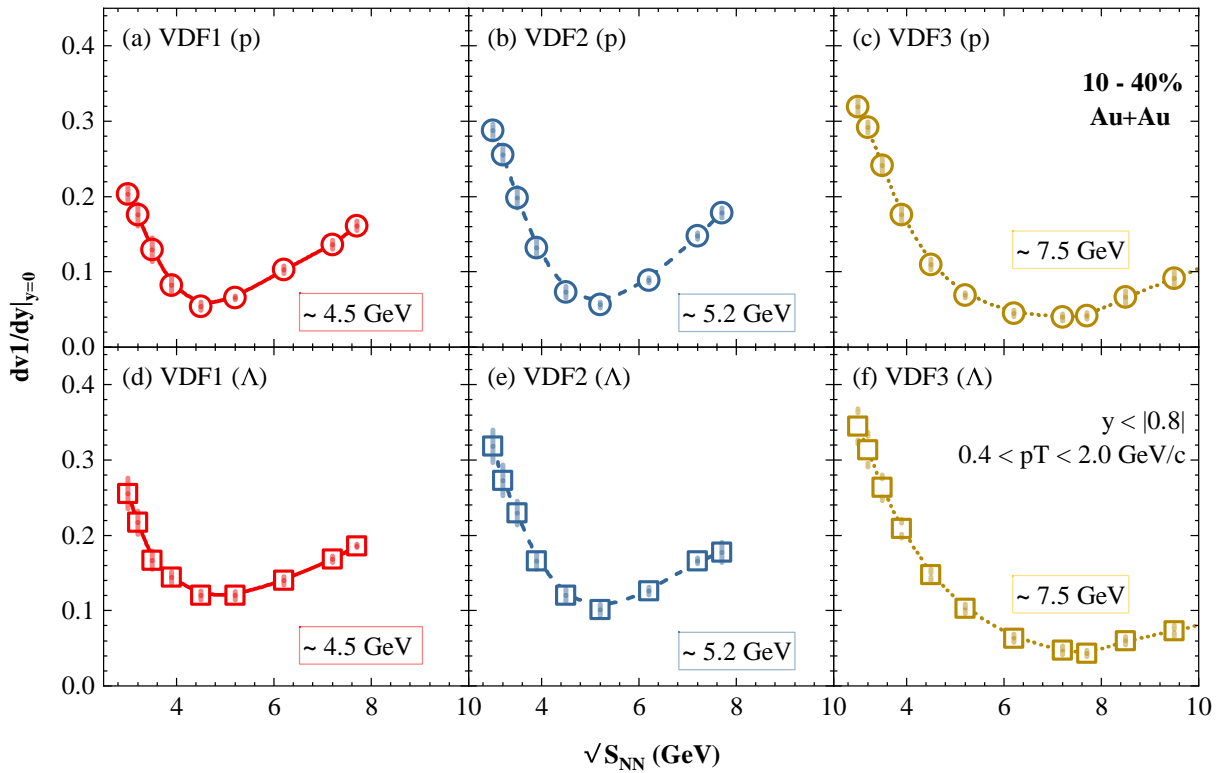


FIG. 3: Energy dependence of the directed flow slope $dv_1/dy|_{y=0}$ for protons (upper panels) and Λ hyperons (lower panels) in the semicentral Au+Au collisions, considering various “QGP-like” VDF EoSs. Points of extremum in the non-monotonic evolution of the slope are highlighted.

of the proton or Λ directed flow strength with the collision energy is experimentally determined, one can infer the presence of a hadron-quark phase transition and its specific location.

The strength of proton directed flow shows a minimum between 11.5 and 19.6 GeV [44], suggesting a possible signature of a first-order phase transition, seems to contradict the findings, e.g., the number-of-constituent quark (NCQ) scaling of elliptic flows of a group of particles [45] and the monotonic energy dependence of net-proton number fluctuations above 10 GeV, which implying the phase-transition of QCD matter very likely occurs at $\sqrt{s_{NN}} < 10$ GeV [46, 47]. Therefore, in Figure 3, we do not show the directed flow slope above 10 GeV.

In conclusions, based on the pure hadronic transport model AMPT-HC, combined with the EoS containing QCD-like phase transition, we studied the proton and Λ directed flow in Au+Au collisions in the FXT energy regime. It is found that the compressed baryon density is somewhat sensitive to the phase transition of nuclear matter. Although our model calculations approximately

constrain the EoS of nuclear matter when compared to experimental data, considering the uncertainties in theoretical model calculations, we propose to investigate the possibility of a hadron-quark first-order phase transition and its specific location by examining whether there are extremum points in the energy dependence of directed flow strength for protons and Λ hyperons, and if so, their specific positions. This involves using both protons and Λ hyperons as dual observables for consistency checks across different particles and reduces the dependency of the results on the uncertainty of the Lambda hyperon potential. To make a long story short, the presence of extremum points in the beam energy dependence of the directed flow strength of protons and Λ hyperons, the consistency of these extremum points, and their specific locations can serve as new observables for the hadron-quark phase transition in heavy-ion collisions.

This work is supported by the National Natural Science Foundation of China under Grant Nos. 12275322, 12335008 and CAS Project for Young Scientists in Basic Research YSBR-088.

[1] Blaschke, David, et al. Understanding the Origin of Matter: Perspectives in Quantum Chromodynamics.

Springer, 2022.
[2] STAR Collaboration: J. Adams *et al.*, Nucl. Phys. A

- 757**, 102-183 (2005).
- [3] STAR Collaboration: J. Adams *et al.*, Phys. Rev. Lett. **92**, 052302 (2004).
- [4] STAR Collaboration: J. Adams *et al.*, Phys. Rev. Lett. **95**, 122301 (2005).
- [5] M. M. Aggarwal *et al.*, arXiv:1007.2613 (2010).
- [6] H. Stöcker, Nucl. Phys. A **750**, 121-147 (2005).
- [7] M. A. Stephanov, K. Rajagopal, and E. V. Shuryak, Phys. Rev. Lett. **81**, 4816 (1998).
- [8] S. Singha, P. Shanmuganathan, and D. Keane, Adv. High Energy Phys. **2016**, 2836989 (2016).
- [9] STAR Collaboration: J. Adam *et al.*, Phys. Rev. C **99**, 064905 (2019).
- [10] Y. Nara, T. Maruyama, and H. Stöcker, Phys. Rev. C **102**, 024913 (2020).
- [11] L. Kumar, and D. Keane, Pramana - J. Phys. **84**, 773-786 (2015).
- [12] CBM Collaboration: T. Ablyazimov *et al.*, Eur. Phys. J. A **53**, 60 (2017).
- [13] C. Sturm, B. Sharkov, and H. Stöcker, Nucl. Phys. A **834**, 682c (2010).
- [14] V. Kekelidze *et al.*, Nucl. Phys. A **956**, 846 (2016).
- [15] J. C. Yang *et al.*, Nuclear Instruments and Methods in Physics Research Section B: Beam Interactions with Materials and Atoms, **317**, 263-265 (2013).
- [16] J-PARC Heavy-Ion Collaboration H. Sako *et al.*, Nucl. Phys. A **931**, 1158 (2014); **956**, 850 (2016).
- [17] H. Stöcker, and W. Greiner, Phys. Rep. **137**, 277 (1986).
- [18] P. Danielewicz, R. Lacey, and W. G. Lynch, Science **298**, 1592 (2002).
- [19] Y. Nara, A. Ohnishi, Phys. Rev. C **105**(1), 014911 (2022).
- [20] M. O. Kuttan, A. Motornenko, J. Steinheimer, H. Steinheimer, Y. Nara, M. Bleicher, Eur. Phys. J. C **82**(5), 427 (2022).
- [21] Y. Nara, H. Niemi, J. Steinheimer, and H. Stöcker, Phys. Lett. B **769**, 543 (2017).
- [22] A. Sorensen, V. Koch, Phys. Rev. C **104**, 034904 (2021).
- [23] A. M. Poskanzer and S. A. Voloshin, Phys. Rev. C **58**, 1671 (1998).
- [24] Gao-Chan Yong, Zhi-Gang Xiao, Yuan Gao, Zi-Wei Lin, Phys. Lett. B **820**, 136521 (2021).
- [25] Zi-Wei Lin, Liang Zheng, Nucl. Sci. Tech. **32**, 113 (2021).
- [26] Zi-Wei Lin, Che Ming Ko, Bao-An Li, Bin Zhang, Subrata Pal, Phys. Rev. C **72**, 064901 (2005).
- [27] Yongseok Oh, Zi-Wei Lin, Che Ming Ko, Phys. Rev. C **80**, 064902 (2009).
- [28] Gao-Chan Yong, Bao-An Li, Zhi-Gang Xiao, and Zi-Wei Lin, Phys. Rev. C **106**, 024902 (2022).
- [29] Gao-Chan Yong, Phys. Rev. D **108**, L091507 (2023).
- [30] Gao-Chan Yong, Phys. Lett. B **848**, 138327 (2024).
- [31] L. D. Landau, Nucl. Phys. **3**, 127 (1957).
- [32] G. Baym and S. A. Chin, Nucl. Phys. A **262**, 527 (1976).
- [33] J. Steinheimer, A. Motornenko *et al.*, Eur. Phys. J. C **82**, 911 (2022).
- [34] J. Steinheimer, J. Auvinen, H. Petersen, M. Bleicher, and H. Stöcker, Phys. Rev. C **89**, 054913 (2014).
- [35] V. P. Konchakovski, W. Cassing, Yu. B. Ivanov, and V. D. Toneev, Phys. Rev. C **90**, 014903 (2014).
- [36] Yu. B. Ivanov and A. A. Soldatov, Phys. Rev. C **91**, 024915 (2015).
- [37] Yasushi Nara, Harri Niemi, Akira Ohnishi, and Horst Stöcker, Phys. Rev. C **94**, 034906 (2016).
- [38] Dirk H. Rischke, YarişPürsün, Joachim A. Maruhn, Horst Stöcker, Walter Greiner, APH N.S., Heavy Ion Physics **1**, 309 (1995).
- [39] J. Steinheimer, A. Motornenko, A. Sorensen *et al.*, Eur. Phys. J. C **82**, 911 (2022).
- [40] STAR Collaboration: M. S. Abdallah *et al.*, Phys. Lett. B **827**, 137003 (2022).
- [41] STAR Collaboration: M. S. Abdallah *et al.*, Phys. Rev. C **103**, 034908 (2021).
- [42] STAR Collaboration: L. Adamczyk *et al.*, Phys. Rev. Lett. **120**, 062301 (2018).
- [43] STAR Collaboration: L. Adamczyk *et al.*, Phys. Rev. Lett. **112**, 162301 (2014).
- [44] STAR Collaboration: L. Adamczyk *et al.*, Phys. Rev. Lett. **112**, 162301 (2014).
- [45] STAR Collaboration: L. Adamczyk *et al.*, Phys. Rev. C **88**, 014902 (2013).
- [46] STAR Collaboration: J. Adam *et al.*, Phys. Rev. Lett. **126**, 092301 (2021).
- [47] STAR Collaboration: M. S. Abdallah *et al.*, Phys. Rev. Lett. **128**, 202303 (2022).